Communicated by Gordon M. Shepherd

A Canonical Microcircuit for Neocortex

Rodney J. Douglas
Kevan A.C. Martin
David Whitteridge
MRC Anatomical Neuropharmacology Unit, Department of Pharmacology, South Parks Road, Oxford OX1 3QT, England

We have used microanatomy derived from single neurons, and *in vivo* intracellular recordings to develop a simplified circuit of the visual cortex. The circuit explains the intracellular responses to pulse stimulation in terms of the interactions between three basic populations of neurons, and reveals the following features of cortical processing that are important to computational theories of neocortex. First, inhibition and excitation are not separable events. Activation of the cortex inevitably sets in motion a sequence of excitation and inhibition in every neuron. Second, the thalamic input does not provide the major excitation arriving at any neuron. Instead the intracortical excitatory connections provide most of the excitation. Third, the time evolution of excitation and inhibition is far longer than the synaptic delays of the circuits involved. This means that cortical processing cannot rely on precise timing between individual synaptic inputs.

1 Introduction

The uniformity of the mammalian neocortex (Hubel and Wiesel 1974; Rockel *et al.* 1980) has given rise to the proposition that there is a fundamental neuronal circuit (Creutzfeldt 1977; Szentágothai 1978) repeated many times in each cortical area. Here we provide evidence for such a canonical circuit in cat striate cortex, and model its form and functional attributes.

The microcircuitry of the striate cortex of the cat is by far the best understood of all cortical areas. The anatomical organization that has emerged from studies (Gilbert and Wiesel 1979; Martin 1988) of neuronal morphology and immunochemistry is one of stereotyped connections between different cell types: pyramidal cells connect principally to other pyramidal cells, and the smooth cells connect principally to pyramidal cells. Pyramidal cells are excitatory; smooth cells are GABAergic and thought to be inhibitory. Some neurons of both types are driven directly by thalamic input and others indirectly. We used these findings and those described below to develop the simplest neuronal circuit that

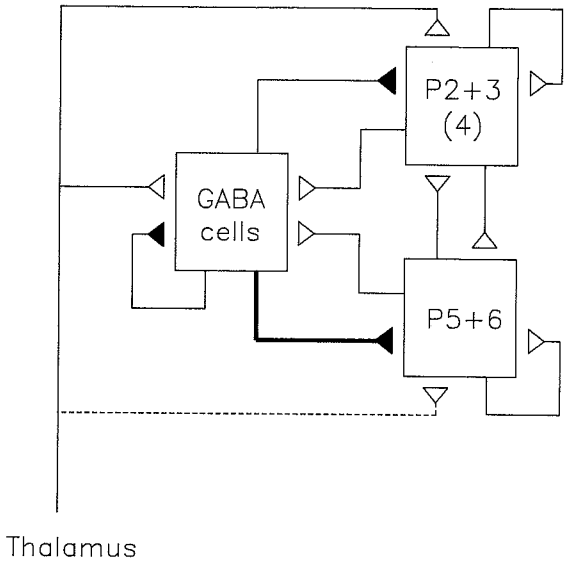

Figure 1: Model of cerebral cortex that successfully predicts the intracellular responses of cortical neurons to stimulation of thalamic afferents. Three populations of neurons interact with one another: one population is inhibitory (*GABA cells*, solid synapses), and two are excitatory (open synapses), representing superficial ($P2+3$) and deep ($P5+6$) layer pyramidal neurons. The layer 4 spiny stellate cells are incorporated with the superficial group of pyramids. Each population receives excitatory input from the thalamus, which is weaker (dashed line) to deep pyramids. The inhibitory inputs activate both $GABA_A$ and $GABA_B$ receptors on pyramidal cells. The thick line connecting *GABA* to $P5+6$ indicates that the inhibitory input to the deep pyramidal population is relatively greater than that to the superficial population. However, the increased inhibition is due to enhanced $GABA_A$ drive only. The $GABA_B$ inputs to $P5+6$ is similar to that applied to $P2+3$.

showed analogous functional behavior to that which we observed in our intracellular recordings (Fig. 1).

2 Cortical Model

The model circuit consisted of populations of neurons that interacted with one another. The behavior of each population was modeled by a single "cell" that represented the average response of the neurons be-

longing to that population. The action potential discharge was treated as a rate-encoded output rather than discrete spike events. The populations excited or inhibited one another by inducing changes in the average membrane potential of their target populations, after a transmission delay. The relaxation of the membrane potential was governed by a membrane time constant. The magnitude of excitation or inhibition was determined by the product of the input population's discharge rate, a synaptic coupling coefficient, and a synaptic driving potential. The discharge rate was a thresholded hyperbolic function of the average membrane potential. The synaptic coupling coefficient incorporated the fraction of all synaptic input that was derived from a particular source population, the average efficacy of a synapse from that source, and the sign of its effect (either positive or negative). The synaptic driving potential was the difference between the average membrane potential and the appropriate synaptic reversal potential. The number and characteristics of the populations, and the functional weighting of their interconnections, were optimized by comparing the performance of the model with that of the cortex itself, as described below. The model was programmed in TurboPascal and run on a 8-MHz 80286/287 AT-type computer, which computed a typical model response of 400 msec in 30 sec.

3 Intracellular Recordings

Neurons were recorded from the postlateral gyrus of the striate visual cortex (area 17) of anesthetized, paralyzed cats (Martin and Whitteridge 1984; Douglas *et al.* 1988), while continuously monitoring vital signs. Glass micropipettes were filled with 2 *M* K citrate, or a 4% buffered solution of horseradish peroxidase (HRP) in 0.2 *M* KCl. GABA agonists and antagonists were applied ionophoretically via a multibarrel pipette using a *Neurophore* (Medical Systems Inc.). The intracellular electrode was mounted in a "piggy-back" configuration on a multibarrel ionophoretic pipette. The tip of the recording electrode was separated from the tips of the ionophoretic barrels by 10–20 μm. Receptive fields of the cortical neurons were first plotted in detail by hand, and then intracellular recordings were made while stimulating the optic radiation (OR) above the lateral geniculate nucleus via bipolar electrodes (0.2–0.4 msec, 200–400 μA). A control period of 100 msec, followed by 300 msec of the intracellular response to OR stimulation, was averaged over up to 32 trials. We used electrical pulse stimulation as a test signal both because it simplifies the analysis of systems, and because it permits the canonical microcircuit hypothesis to be tested in the many cortical areas whose natural stimulus requirements are not yet known. Where possible, HRP was injected intracellularly following data collection to enable morphological identification. Twenty HRP-labeled neurons were recovered (Fig. 2).

4 Results and Discussion

In all 53 cells examined, the stimulus pulse induced a sequence of excitation followed by a lengthy (100–200 msec) hyperpolarizing inhibitory postsynaptic potential (IPSP) that inhibited completely any spontaneous action potential discharge. This general pattern has been reported in visual and other cortical areas, and it is currently supposed that the early excitation is due to activation of thalamic afferents, and that the inhibition arises from feed-forward and feedback excitation of cortical smooth cells.

There is strong evidence that inhibition in the cortex involves $GABA_A$ receptors, which can be selectively blocked by bicuculline (Sillito 1975). However, we found that there was also a second GABAergic inhibitory mechanism present *in vivo*, which was insensitive to bicuculline and could be activated by the specific $GABA_B$ agonist, baclofen. Baclofen mediated inhibition has also been observed in *in vitro* cortical preparations (Connors *et al.* 1989).

Both GABAergic mechanisms were incorporated into the model so that $GABA_A$ simulation produced an early inhibition of short duration, while the $GABA_B$ reponse evolved more slowly and had a longer duration. For simplicity, both inhibitory processes behaved linearly. This approximation is reasonable since nonlinear inhibition is not prominent in cat visual cortex (Douglas *et al.* 1988). Using these principles, we were able to model the neuron's response to electrical stimulation by a circuit that consisted simply of two interacting populations: one population of excitatory pyramidal cells and another of inhibitory smooth cells, with thalamic input applied to both populations. However, the temporal forms of the responses obtained from *in vivo* cortical cells were not all similar. For pyramidal cells, which formed the bulk of our HRP-labeled sample, we could discriminate two different temporal patterns of poststimulus response on the basis of the latency to maximum hyperpolarization (Fig. 2). These patterns were not correlated with functional properties such as receptive field type or ordinal position, but were strongly correlated with cortical layer (Fig. 2). Hyperpolarization evolved more slowly in morphologically identified pyramidal neurons of layer 2 and 3 than those located in layers 5 and 6. These data suggested that the pyramidal cells might be involved in two different circuits, one for superficial layers (2 and 3), and another for deep layers (5 and 6). Consequently, the model was expanded to incorporate these two populations. Unfortunately, we did not label any spiny stellate cells, which are found only in layer 4. However, the output of spiny stellate cells is directed to the superficial layers as well as layer 4 (Martin and Whitteridge 1984), and so we assumed that they should be incorporated with the population of superficial pyramids. We also assumed that the superficial and deep populations should have similar rules of interconnection. By exploring the properties of the expanded

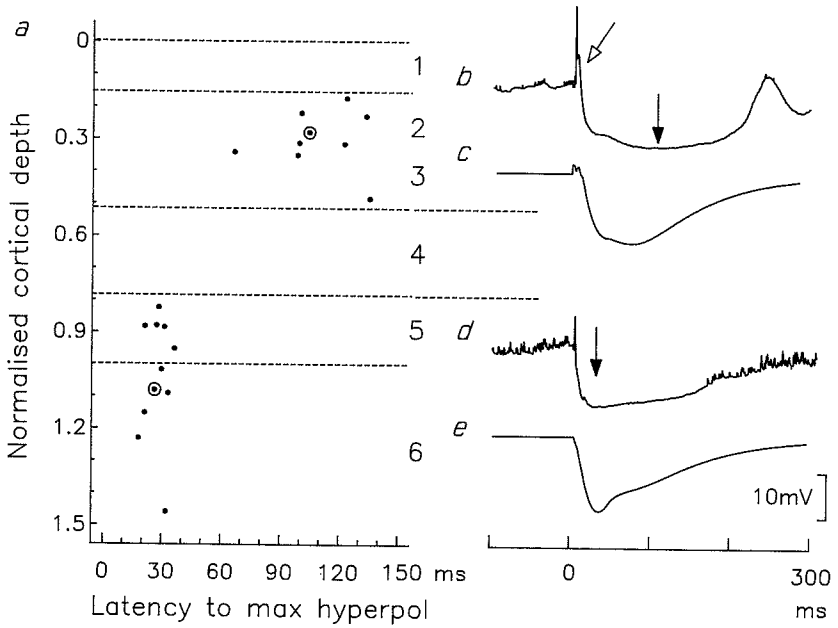

Figure 2: Correlation of cortical layer with the pattern of the intracellular responses to stimulation of the optic radiation. (a) Hyperpolarization evolved more slowly in morphologically identified pyramidal neurons of layer 2 and 3 than those located in layers 5 and 6. (b,d) (modeled in c, e) Latencies to maximum hyperpolarization (filled arrows) were measured with respect to the stimulus at $t = 0$. Mean latencies for the two populations were 108.9 ± -7.3 SEM msec ($N = 9$) and 27.5 ± -1.7 msec ($N = 11$). Superficial pyramids [e.g., b, position circled in a always exhibited marked excitation (open arrow), which was less prevalent in deep layers (e.g., d circled in a)]. In this figure, stimulus artifacts removed for clarity. Depths of identified pyramidal cell somata and layer boundaries were measured with respect to cortical surface and then normalized against the layer 5/6 boundary. The model (Fig. 1) predicted qualitatively similar responses to those observed *in vivo* (compare b to c and d to e) if and only if $GABA_A$ inhibition of deep layers was greater than that of superficial layers.

model, we were able to show that the two layers correlated response patterns could be elicited from the same basic circuit by modifying the the relative intensities of $GABA_A$ inhibition applied to the two pyramidal populations. The observed differences in the pattern of response of superficial and deep neurons could be most simply achieved by making the

$GABA_A$ inhibition of the deep pyramidal cells four times stronger than that of the superficial cells. The strength of $GABA_B$ inhibition was the same in both layers. This configuration (Fig. 1) of the model provided the best fit to the biological data. Alternative combinations of populations and coupling coefficients were markedly less successful in simulating the biological data.

Having established the basic configuration, we then modeled the affect of altering the weightings of the inhibitory (GABAergic) connections. The predictions were tested experimentally by recording the intracellular pulse response during ionophoretic application of various GABA agonists and antagonists. These drugs were applied directly to the recorded cell via a multibarrel ionophoretic micropipette that was mounted on the shank of the intracellular pipette. The close agreement between the predicted and the experimental results are shown in Figure 3.

The performance of the model depends on the coupling between the pyramidal and smooth cells, and this suggests that excitation and inhibition are not separable events. Activation of the cortex inevitably sets in motion a sequence of excitation and inhibition in every neuron. Moreover, the time evolution of excitation and inhibition is far longer than the synaptic delays of the circuits involved. In particular, the large component of the inhibition derives from the $GABA_B$-like process that extends over some 200 msec. This means that cortical processing cannot rely on precise timing between individual synaptic inputs.

The model also predicted that the excitation due to intracortical connections would greatly exceed that of the thalamic afferents, which provide the initial excitation. This amplification of excitation is a consequence of the intracortical divergence (Gilbert and Wiesel 1979; Martin 1988) of pyramidal cell projections. Thus, thalamic input does not provide the major excitation arriving at any neuron. Instead the intracortical excitatory connections provide most of the excitation. This excitation would grow explosively, but it is gated by inhibition of the pyramids.

It is this intracortical excitatory component that is more strongly inhibited in the deep layers, so the onset of maximum hyperpolarization occurs more rapidly in these cells (compare Fig. 2b and d). The degree to which the intracortical component is normally inhibited can be demonstrated by comparing the form of the excitatory depolarization before and after blockade of $GABA_A$-mediated inhibition (Fig. 4). Bicuculline enhanced predominantly the intracortical excitatory component. This suggests that the $GABA_A$ mechanism is activated by the arrival of the thalamic volley, and that the role of tonic cortical inhibition is small.

5 Conclusion

Taken together, these data show that this simple model can provide a remarkably rich description of the average temporal behavior of

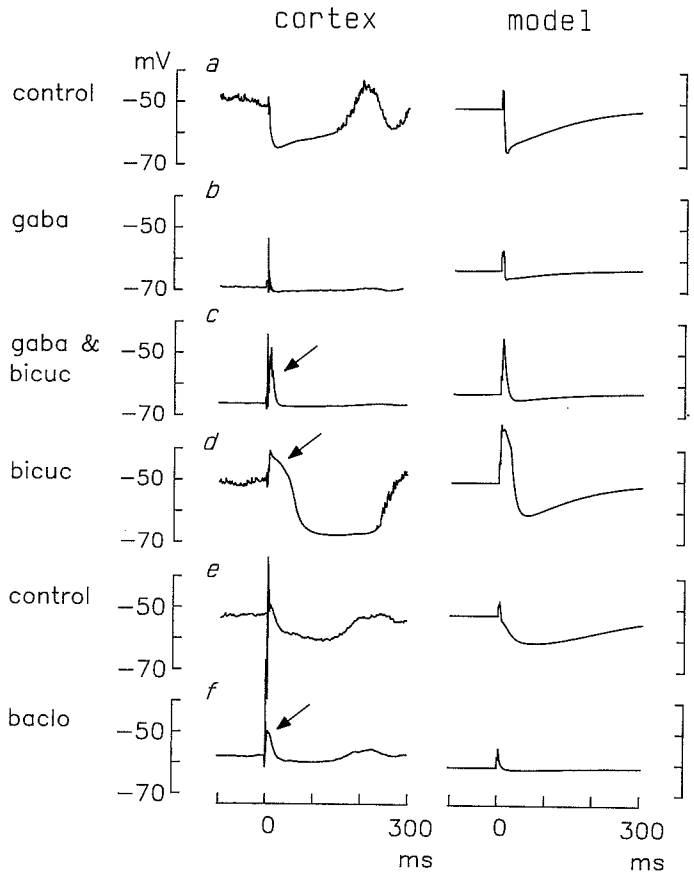

Figure 3: Comparison of predictions of the model with experimental results following modification of synaptic weights. To simulate the localized effect of ionophoresis, manipulations of the model affected only a small subset of P2+3 or P5+6 cells (Fig. 1). (a) Observed and predicted control response of a deep cell. (b) Sustained GABA ejection (Sigma, 0.5M, 70 nA) hyperpolarized the membrane of this cell so reducing the stimulus-induced hyperpolarization. (c) Additional application of $GABA_A$ antagonist bicuculline (Sigma, 100 mM, 200 nA) did not reverse the GABA-induced hyperpolarization, but enhanced excitation (arrow). (d) When GABA was removed, bicuculline further enhanced excitation (arrowed), but did not block late hyperpolarization. (e) Control response of a superficial cell. (f) The $GABA_B$ agonist baclofen (Ciba Geigy, 10 mM, 60 nA) hyperpolarized the membrane of this cell, accentuating the early excitation (arrowed).

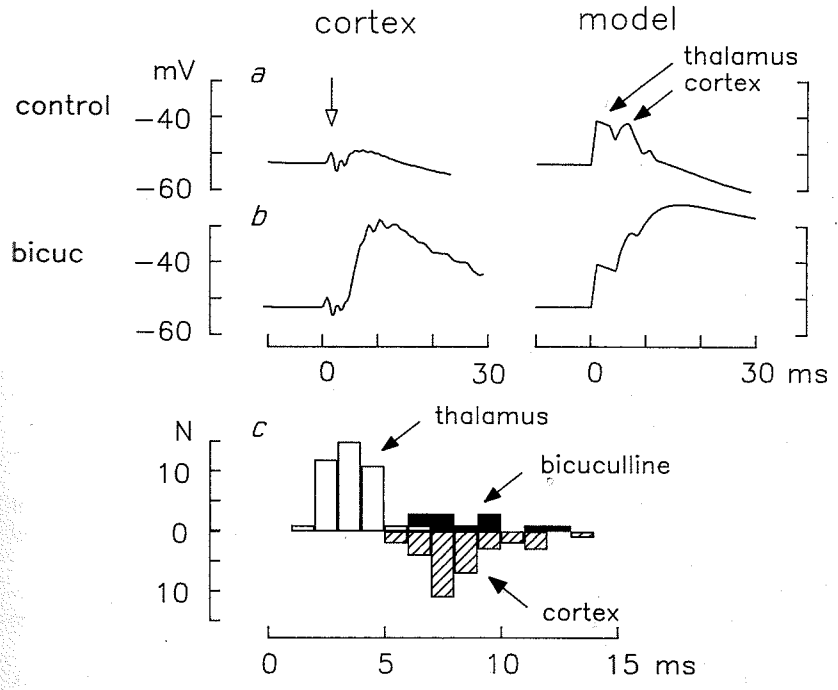

Figure 4: Blocking $GABA_A$ inhibition unmasks intracortical excitation. (a) Observed and predicted excitatory response of a superficial cell during the first 30 msec following the stimulus. Excitatory response was followed by IPSP similar to that seen in Figure 3e. Only initial phase of IPSP is seen in this short time window. Thalamic and intracortical components of excitation are indicated in model response; stimulus artifact is marked with open arrow. (b) Sustained application of bicuculline (0.1M, 100 nA) enhanced the intracortical component, but left the thalamic component largely unaffected. (c) Histogram of experimental results showing that the latency to peak of the bicuculline-affected depolarization (filled bars) corresponds with that of the intracortical component (hatched bars). Both were significantly later than the earliest (thalamic) depolarization (open bins).

populations of cortical neurons when they are activated by pulse stimuli. Because this stimulus is not area specific, the same experimental methods and tests could, in principle at least, be applied to any cortical area, even those whose function is unknown. Similar responses obtained in another cortical area would suggest a basic circuitry similar to that of visual cortex. Furthermore, models of cortical processing that are based

on analogues of neurons (Sejnowski *et al.* 1988) should exhibit responses to pulse activation of their inputs that are qualitatively similar to those reported here.

Acknowledgments

We thank John Anderson for technical assistance, and the E.P. Abrahams Trust for support. R.J.D. acknowledges the support of the Guarantors of *Brain*, and the SA MRC.

References

Connors, B. W., Malenka, R. C., and Silva, L. R. 1988. Two inhibitory postsynaptic potentials, and $GABA_A$ and $GABA_B$ receptor-mediated responses in neocortex of rat and cat. *J. Physiol.* **406**, 443–468.

Creutzfeldt, O. D. 1977. Generality of the functional structure of the neocortex. *Naturwissenschaften* **64**, 507–517.

Douglas, R. J., Martin, K. A. C., and Whitteridge, D. 1988. Selective responses of visual cortical cells do not depend on shunting inhibition. *Nature (London)* **332**, 642–644.

Gilbert, C. D., and Wiesel, T. N. 1979. Morphology and intracortical projections of functionally characterised neurons in the cat visual cortex. *Nature (London)* **280**, 120–125.

Hubel, D. H., and Wiesel, T. N. 1974. Uniformity of monkey striate cortex: A parallel between field size, scatter, and magnification factor. *J. Comp. Neurol.* **158**, 295–305.

Martin, K. A. C. 1988. From single cells to simple circuits in the cerebral cortex. *Q. J. Exp. Physiol.* **73**, 637–702.

Martin, K. A. C., and Whitteridge, D. 1984. Form, function, and intracortical projections of spiny neurones in the striate visual cortex. *J. Physiol.* **353**, 463–504.

Rockel, A. J., Hiorns, R. W., and Powell, T. P. S. 1980. The basic uniformity in structure of the neocortex. *Brain* **103**, 221–244.

Sejnowski, T. J., Koch, C., and Churchland, P. S. 1988. Computational neuroscience. *Science* **241**, 1299–1306.

Sillito, A. M. 1975. The contribution of inhibitory mechanisms to the receptive field properties of neurones in the striate cortex of the cat. *J. Physiol.* **250**, 387–304.

Szentágothai, J. 1978. The neuron network of the cerebral cortex: A functional interpretation. *Proc. R. Soc. (London) Ser. B* **201**, 219–248.

Received 13 July 1989; accepted 2 October 1989.